

Some physical properties of Ga₂Te₅ single crystals

M.M. Nassary*, M.K. Gerges, H.T. Shaban, A.S. Salwa

Physics Department, Faculty of Science, South Valley University, Qena, Egypt

Received 5 May 2003; accepted 18 May 2003

Abstract

Single crystals of Ga₂Te₅ were prepared in our laboratory by a special modified Bridgman technique method. Measurements of the electrical conductivity and Hall effect between 268 and 503 K were carried out on Ga₂Te₅ samples in two crystallographic directions (parallel and perpendicular to the *c*-axis). The Hall coefficient is positive and varies with the crystallographic direction. A unique mobility behaviour and strong anisotropy in the carrier mobility were observed. Also, the present investigation involves the thermoelectric power measurements of Ga₂Te₅ samples in the wide range 170–511 K, when the direction of the temperature gradient is parallel to the layer planes. The combination of the electrical and thermal measurements in the present investigation makes it possible to find various physical parameters such as carrier mobilities, effective masses of free charge carriers (m_p^* , m_n^*), diffusion coefficients (D_p , D_n) and diffusion lengths (L_p , L_n), as well as the relaxation time (τ_p , τ_n) and to reveal the general behaviour of this semiconductor.

© 2003 Published by Elsevier Science B.V.

Keywords: Ga₂Te₅; Hall coefficient; Thermoelectric power

1. Introduction

Crystalline materials with a high anisotropy of physical properties have attracted ever growing attention recently and of particular interest in this connection are the (*A*^{III}*B*^{VI}-type) semiconductors compounds. Characteristic of these crystals is the existence of a great number of diverse structural types very different in their physical properties.

Ga₂Te₅ is an achalcogenide binary compound. The phase diagram of Ga–Te system has been investigated by differential thermal analysis and direct observation of melting points under control to pressures 10⁻⁴–7 mm Hg [1–3]. The earlier

phase diagram determination was compiled by Hansen and Anderko [4] based on experimental results by Klemm and Vogl [5]. Klemm and Vogl identified two compounds (GaTe, Ga₂Te₃) and expected another polytelluride would exist in many countries in the Te-rich region because the longest thermal arrest was observed at 75% Te. Newman et al. [1] reported two other compounds (Ga₃Te₂, GaTe₃), unstable at room temperature, by X-ray analysis. Alapini et al. [2] published results obtained from DTA and X-ray studies and they were in agreement with those of Klemm and GaTe, Ga₂Te₃, Ga₂Te₅ were stable compounds.

After Antonopoulis et al. [6] identified another compound, Ga₃Te₄, by electron microscope, four stoichiometric compounds, GaTe, Ga₃Te₄, Ga₂Te₃ and Ga₂Te₅, were accepted and confirmed

*Corresponding author.

E-mail address: nassary_99@yahoo.com (M.M. Nassary).

by recent DTA works done by Blachnik and Irlé [7], and by Tschirner et al. [8]. The new phase diagram of Ga–Te system was reported by Levinsky et al. [9].

The Ga_2Te_5 crystal structure has a Pearson symbol (tI14) and space group (I4/m) [10]. Deiseroth and Amann [11] found that Ga_2Te_5 contains chains of trans-edge-sharing GaTe_4 tetrahedra and additional Te-atoms according to formulation $\text{Te}[\text{GaTe}_{4/2}]_2$ ($a = 792.9$ pm, $b = 792.9$ pm and $c = 685.5$ pm). The gallium compound forms a body-centered tetragonal structure (see Fig. 1.) in which infinite chains $[\text{GaTe}_{4/2}]_\infty$ of edge-linked GaTe_4 tetrahedra are held together by interchain Te atoms in a square-planar coordination of Te atoms from the four surrounding chains.

Deiseroth and Amann [11] studied the polymorphism structural relations and homogeneity ranges of M_2Te_5 ($\text{M} = \text{Al}, \text{Ga}, \text{In}$). Electronic structure of semiconducting compounds Re_2Te_5 , Ga_2Te_5 , K_2SnTe_5 was studied by Bullet [12]. The three crystal structures have in common Te in a quasi-planar environment of four Te neighbours.

In this present work, we intend to investigate the electrical conductivity, Hall effect and their temperature dependence and also the thermo-electric power phenomena of Ga_2Te_5 compounds. From this study, we could determine the main

physical parameters such as the energy gap, the depth of the impurity level, the Hall coefficient, conductivity type, the diffusion coefficient, the diffusion length, the scattering mechanism of the charge carriers and their concentration, the mobility, the effective mass and the lifetime of both majority and minority carriers.

2. Experimental procedures

2.1. Crystal growth

High quality of Ga_2Te_5 single crystal has been grown from melt in our laboratories by a special modified Bridgman technique. The growth method and the experimental apparatus have been described in detail elsewhere [13]. The purities of the materials used were as follows, Ga 99.999%, Aldrich mark and Te 99.999%, Aldrich mark. Stoichiometric quantities of the constituent elements (2.324 gm Ga and 10.6333 gm Te) representing 17.935% Ga and 82.064% Te were used as starting materials. The appropriate amounts were first sealed in quartz ampoules at a pressure of 10^{-6} Torr. The quartz ampoule was washed with pure alcohol and hot distilled water and then coated with a thin layer of graphite to prevent contamination of the charge on the internal surface of the ampoule. Individual components were weighed using an electric balance, which was characterized with sensitivity equal to 10^{-4} gm (Sartorius Mark). The reaction vessel was heated to about 814 K under thorough agitation to ensure complete mixing of the components. The ampoule was held in the hot zone of a three-zone tube furnace for about 24 h and then allowed to be drawn at a very slow rate (1.2 mm h^{-1}) to enter the middle zone where the crystallization temperature of the compound was reached. This temperature was 754 K according to the phase diagram reported by Levinsky et al. [9]. Finally, the ampoule entered the last zone in the furnace where the temperature was below the melting point. Such a process requires at least 15 days. The resulting single crystal obtained by the above procedure was 2 cm in length and 1.5 cm in diameter. The results of the X-ray analysis (which was done at the

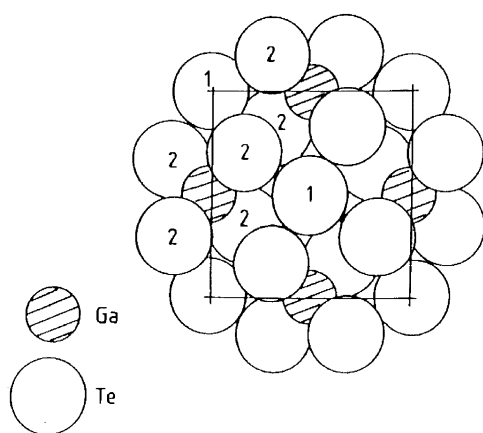


Fig. 1. The Ga_2Te_5 structure, showing the projection down the c -axis of Te atoms at $z = 0$ and $z = 0.5$ and Ga atoms at $z = 0.25$. Te(1) atoms are 4-fold-planar coordinated by Te(2) atoms in the surrounding $[\text{GaTe}_{4/2}]_\infty$ infinite chains.

Central Metallurgical Research and Development Institute (CMRDI), Egypt) revealed the presence of a good crystalline phase without any secondary phases.

2.2. Measuring technique

For studying the electrical conductivity and Hall effect, the sample was prepared in a rectangular shape. In this way, the length of the sample was made 3 times its width to avoid Hall voltage drop. After going through the polishing processes, the sample's dimensions were $11.95 \times 3.5 \times 1.1 \text{ mm}^3$. If we refer to the current, the optic axis coinciding with the c -axis of the crystal and the applied magnetic field with the symbols J , C and H respectively, we can sum up the conditions of the measurements when the current was parallel to the c -axis as $J \parallel C \perp H$ and when the current flows perpendicular to the c -axis as $J \perp C \parallel H$. Measurements were done with the help of a Pyrex glass cryostat, which was designed in our laboratories by Hussein [14] for this purpose, and a sensitive potentiometer (UJ33E mark). The cryostat is used as a holder, evacuated container for liquid nitrogen (in case of low measurements), and as a support to the electric heater (for high temperature measurements). By using Edward rotary pump, we evacuated the cryostat (10^{-3} Torr) for protecting the sample from the water vapour condensation and oxidation. Copper–constantan thermocouple was used for measuring the environment temperature of the sample. Silver paste was used as an ohmic contact by pointing the cleaved cherry red sample. An intermediate magnetic field ($\approx 5 \text{ kg}$) supplied from Oxford electromagnet (N117 type) was used.

In the thermoelectric power (TEP) measurements, an evacuated calorimeter ($\sim 10^{-3}$ Torr) was used to protect the sample from oxidation and water vapour condensation at high and low temperatures respectively. The calorimeter has two heaters. The outer heater (the external source) discharges its heat slowly to the specimen environment. The inner heater (connected to the lower end of the crystal) was made purposely to properly control the temperature and its gradient along the specimen.

The TEP is calculated at different temperatures by dividing the magnitude of the thermovoltage difference across the crystal by the temperature difference between the hot and cold ends, where the thermovoltage is measured by a sensitive potentiometer (UJ33E mark).

3. Results and discussion

3.1. Electrical conductivity and the Hall coefficient

Interesting physical phenomenon in Ga_2Te_5 layer semiconductor includes a strong anisotropy of electrical conductivity. We investigate in great details, the anisotropy of electrical properties, and particularly deal with the changes in Hall coefficient and Hall mobility as well as electrical conductivity (σ) of Ga_2Te_5 in the temperature ranges extending from 268 to 503 K. Fig. 2 gives the temperature dependence of electrical conductivity parallel (σ_{\parallel}) and perpendicular (σ_{\perp}) to the layers of Ga_2Te_5 single crystal, where the intrinsic

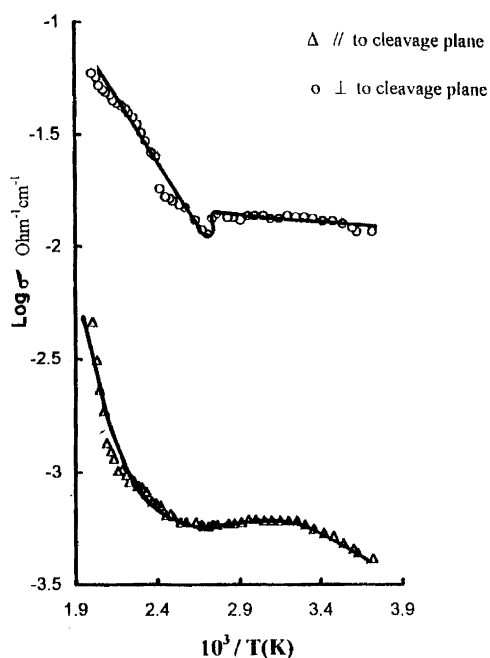


Fig. 2. Temperature dependence of the electrical conductivity for Ga_2Te_5 .

region in this sample appears at 384 K for σ_{\parallel} and at 377 K for σ_{\perp} . The transition region lies in the temperature range 333–384 K for σ_{\parallel} and 357–377 K for σ_{\perp} . The energy gaps $\Delta E_{g\parallel}$ and $\Delta E_{g\perp}$ assessed from the graph of $\text{Log}(\sigma) = F(10^3/T)$ are 1.77 eV and 0.46 eV respectively. The value of $\Delta E_{g\parallel} = 1.77$ eV agrees with the values obtained from electronic structure calculations ($\Delta E_g = 1.7$ eV) by Bullent [12]. The room temperature conductivity of this sample is $5.8 \times 10^{-4} \Omega^{-1} \text{cm}^{-1}$ parallel to the cleavage plane and $13 \times 10^{-3} \Omega^{-1} \text{cm}^{-1}$ perpendicular to the cleavage plane. Fig. 2 shows that the conductivity perpendicular to the layers plane differs from that parallel to it, suggesting a great anisotropy. Fig. 3 illustrates an examination of the anisotropy of the electrical conductivity at all the temperature ranges of investigation. The ratio $\sigma_{\perp}/\sigma_{\parallel}$ seems to be fairly constant and equals 25.52. Presence of such anisotropies here can be partly or wholly attributed to interlayer macroscopic defects and/or planes of precipitates, as studied by Gamal et al. [15]. Fig. 4 shows the relation between $\text{Log}(R_H T^{3/2})$ and $10^3/T$. This curve is divided into two regions: The first part of low temperatures, $R_{H\parallel} T^{3/2}$ and $R_{H\perp} T^{3/2}$, grow slowly with respect to the temperature and reach maximum value of 3×10^{10} and 1.26×10^8 at 388 K, respectively. This region indicated the extrinsic region and from this we calculated the position of the acceptor level to be $\Delta E_{a\parallel} = 0.33$ eV and

$\Delta E_{a\perp} = 0.19$ eV. In the second region above 388 K, a rapid decrease was observed as the temperature increases for $R_{H\parallel} T^{3/2}$ and $R_{H\perp} T^{3/2}$. This region indicated the intrinsic region and from this we calculated the energy gap $\Delta E_{g\parallel} = 1.79$ eV, $\Delta E_{g\perp} = 0.47$ eV). These values agree with that deduced from the conductivity data. The Hall coefficients at room temperature is evaluated as

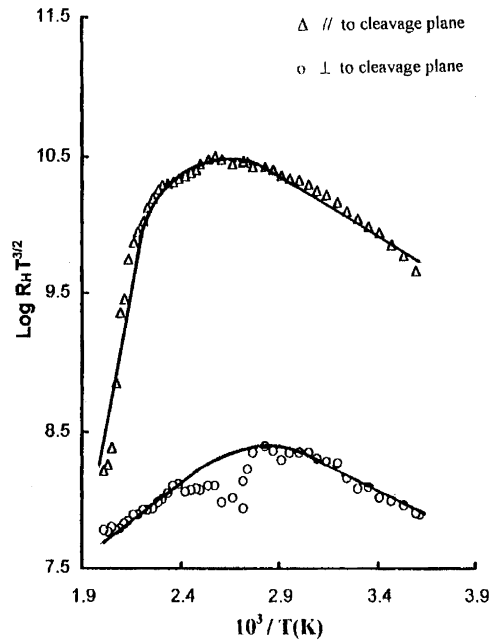


Fig. 4. The relation between $R_H T^{3/2}$ and $10^3/T$ of Ga_2Te_5 .

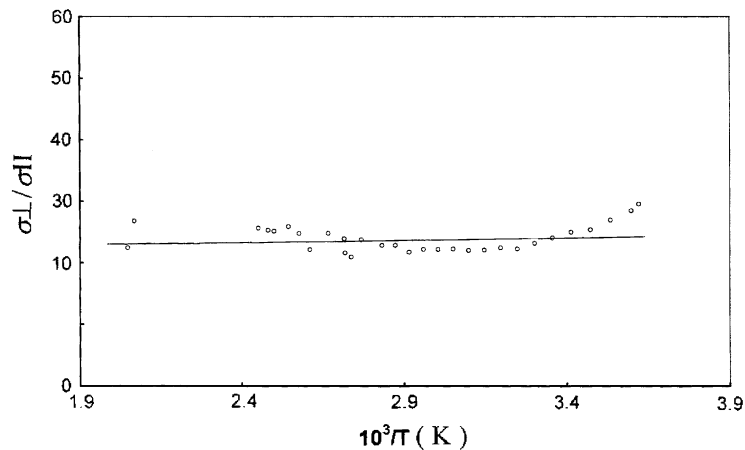


Fig. 3. Temperature dependence of the anisotropic factor for Ga_2Te_5 .

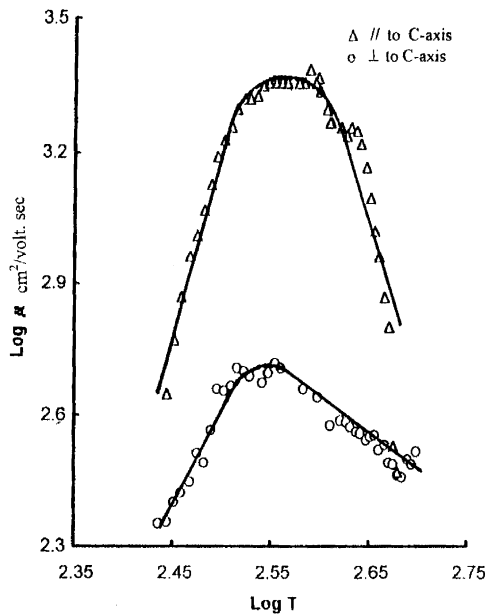


Fig. 5. The behaviour of Hall mobility as a function of temperature for Ga_2Te_5 .

$R_{H\parallel} = 20 \times 10^5 \text{ cm}^3/\text{C}$ and $R_{H\perp} = 23 \times 10^3 \text{ cm}^3/\text{C}$. Hence their ratio, $R_{H\perp}/R_{H\parallel}$ is 0.0115. It can be noticed that $R_{H\parallel}$ is higher in magnitude than $R_{H\perp}$ in the temperature range under study. The positive sign of the R_H -values signifies that Ga_2Te_5 has a p-type nature over the entire temperature range of investigation. Fig. 5 shows the temperature dependence of charge carrier mobilities. From this curve, we can distinguish three regions. In the first region of low temperatures from 275 to 354 K, mobility $\mu_{H\parallel}$ increases with temperature obeying the law $\mu \propto T^{8.2}$. Such behaviour is characteristic of a scattering mechanism of the charge carriers with ionized impurities. In the second region from 354 to 484.5 K, mobility $\mu_{H\parallel}$ nearly has a constant value with increasing temperature until 384.5 K, which corresponds to the transition region, after which the third region begins. At high temperature ranges (384–501 K) mobility $\mu_{H\parallel}$ decreases with increasing temperature according to the law $\mu \propto T^{-10}$. This leads to the assumption that lattice scattering dominates and that the impurity concentration has little effect on the mobility.

Mobility $\mu_{H\perp}$ has the same behaviour. In the temperature, range 268–360 K the mobility $\mu_{H\perp}$ increases as temperature grows obeying the law $\mu_{H\perp} \propto T^{3.53}$. This leads to the assumption that scattering is caused by the ionized and unionized acceptor atoms. In the high temperature range (360–501 K) mobility $\mu_{H\perp}$ decreases with increasing temperature according to the law $\mu_{H\perp} \propto T^{1.62}$. This behaviour leads to phonons scattering. At room temperature Hall mobility along the layers $\mu_{H\parallel}$ is equal to $5011.8 \text{ cm}^2/\text{V s}$ and that normal to the layers $\mu_{H\perp}$ is equal to $309.3 \text{ cm}^2/\text{V s}$. The typical behaviour of the carrier concentration as a function of temperature is illustrated in Fig. 6. This shows that the concentration decreases when the temperature increases at extrinsic region, while it increases with temperature in the intrinsic region.

For the intrinsic region the following formula is applied [16]:

$$P_i = (N_c N_v)^{1/2} e^{-\Delta E_g/2KT} = C e^{-\Delta E_g/2KT}. \quad (1)$$

From this relation, the energy gap and the acceptor energy level were calculated and found to be in a good agreement with the values obtained

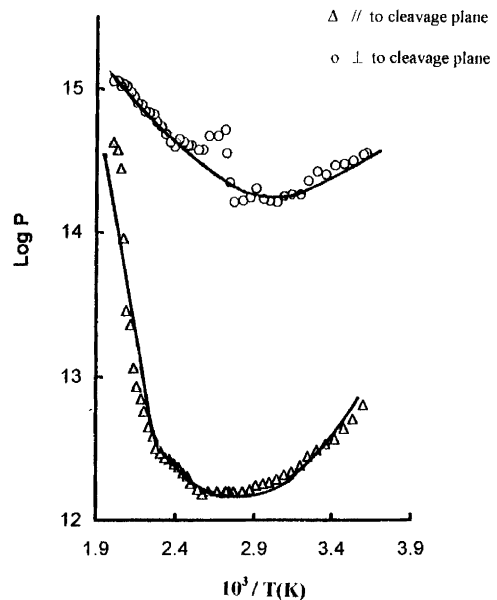


Fig. 6. Variation of carrier concentration with temperature for Ga_2Te_5 .

earlier. From Hall coefficient data, the charge carriers concentration was calculated by using the relation $R_H = 1/pe$, where p is the hole concentration and e is the electron charge. The carrier concentration at room temperature calculated from the $R_{H\perp}$ and $R_{H\parallel}$ values, were $3.09 \times 10^{12} \text{ cm}^{-3}$ and $2.69 \times 10^{14} \text{ cm}^{-3}$, respectively. The variation of the values of the carrier concentration along and perpendicular to the c -axis gives good evidence of the strong anisotropy of the Ga_2Te_5 single crystals and its interesting semiconductor properties.

3.2. Thermoelectric power (TEP)

Gallium chalcogenides have interesting thermoelectric properties and many practical applications [17]. This study may be the first investigation of TEP for Ga_2Te_5 . Measurements of thermal e.m.f of Ga_2Te_5 crystal were carried out when the direction of the temperature gradient is parallel to the layer planes. Measurements covered the temperature ranging from 170 to 511 K.

Fig. 7 illustrates the general mode of variation of TEP with temperature. This was done by plotting the relation between α and $\text{Ln } T$. It is

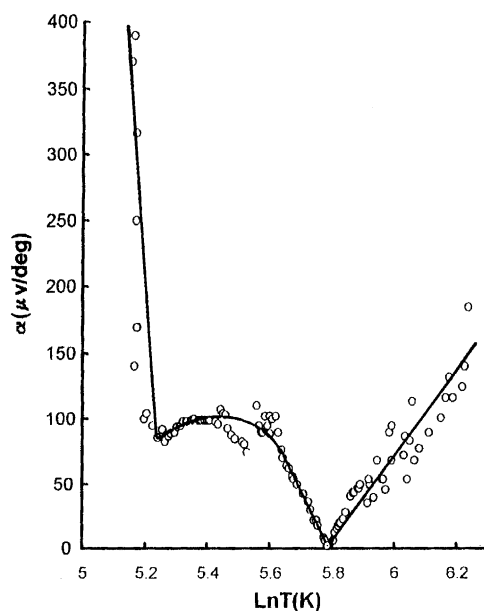


Fig. 7. The relation between α and $\text{Ln } T$ of Ga_2Te_5 .

evident from the figure that, in the intrinsic conduction region ($T > 425$), the absolute value of TEP increases linearly with increasing temperature. At the beginning of the curve TEP decreases rapidly as the temperature is raised reaching value α equal to $82 \mu\text{V/K}$ corresponding to 193 K. Above this temperature, it is noticed that the value of α is almost independent of the temperature up to 275.5 K. At this temperature, the value of α decreases linearly with increasing temperature, in the temperature range 275.5–425 K, reaches a minimum value at α equal to $5 \mu\text{V/K}$ corresponding to 425 K. The room temperature thermoelectric power value for Ga_2Te_5 sample amounted to $50 \mu\text{V/K}$.

Since α has a positive sign over the entire temperature range of investigation, the sample's majority carriers are the holes, i.e. Ga_2Te_5 crystal exhibits p-type conductivity, which is in good agreement with the results reported for Hall effect. The observed large values of thermoelectric power in Ga_2Te_5 samples at low temperature indicate drag of carriers by phonons.

The behaviour of thermoelectric power with temperature in the intrinsic region can be described by the equation of Lauc [18]:

$$\alpha = -\frac{K}{e} \left[\frac{b-1}{b+1} \left(\frac{\Delta E_g}{2KT} + 2 \right) + \frac{1}{2} \ln \left(\frac{m_n^*}{m_p^*} \right)^{3/2} \right], \quad (2)$$

where K is the Boltzmann constant, b is the ratio of the electron to hole mobilities, ΔE_g is the energy gap width, and m_n^*, m_p^* are the effective masses of electrons and holes, respectively. This relationship shows that a plot of α in the intrinsic range as a function of a reciprocal of absolute temperature is a straight line as shown in Fig. 8. The slope of the linear part of this dependence is used to estimate the ratio of the electron and hole mobilities. Taking $\Delta E_{g\parallel} = 1.77 \text{ eV}$ (as obtained from the electrical conductivity and Hall effect data), the ratio $b = \mu_n/\mu_p$ is found to be 1.71. Since $\mu_p = 5011 \text{ cm}^2/\text{V s}$, we can evaluate $\mu_n = 8570 \text{ cm}^2/\text{V s}$. Another important parameter can be deduced with the aid of the obtained values of μ_n and μ_p using the famous Einstein relation [19]; i.e. the diffusion coefficient for both majority and minority carriers (holes and electrons) at room

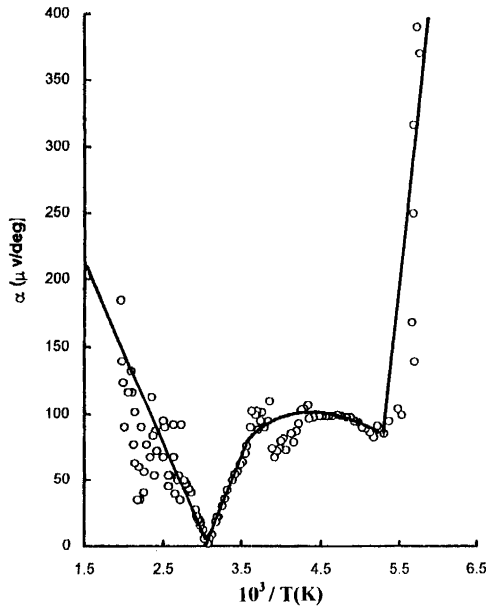


Fig. 8. The relation between α and $10^3/T$ for Ga_2Te_5 .

temperature can be evaluated as $D_p = 125.2 \text{ cm}^2/\text{s}$ and $D_n = 214.25 \text{ cm}^2/\text{s}$, respectively. From the intersection of the curve, the ratio between the effective masses of both electrons and holes can be evaluated as $m_n^*/m_p^* = 1.93 \times 10^{-3}$ and assume that this ratio does not vary with temperature.

Another important relation was suggested by Wilson [20] for application in the extrinsic region:

$$\alpha = \frac{K}{e} \left[2 - \ln \frac{ph^3}{2(2\pi m_p^* KT)^{3/2}} \right]. \quad (3)$$

The above relation is represented graphically in Fig. 7.

Fig. 9 shows the dependence of TEP on carrier concentration for a given Ga_2Te_5 sample. As we have seen, α decreases linearly with the increase of the carrier concentration in the low carrier density region. Calculation of the effective mass of holes from the intersection of the curve yields the value $m_p^* = 82.5 \times 10^{-30} \text{ kg}$.

Combining these values with the above-mentioned results for the ratio m_n^*/m_p^* , one obtains an effective mass of electrons ($m_n^* = 1.5 \times 10^{-31} \text{ kg}$). The mean free time between collisions can be

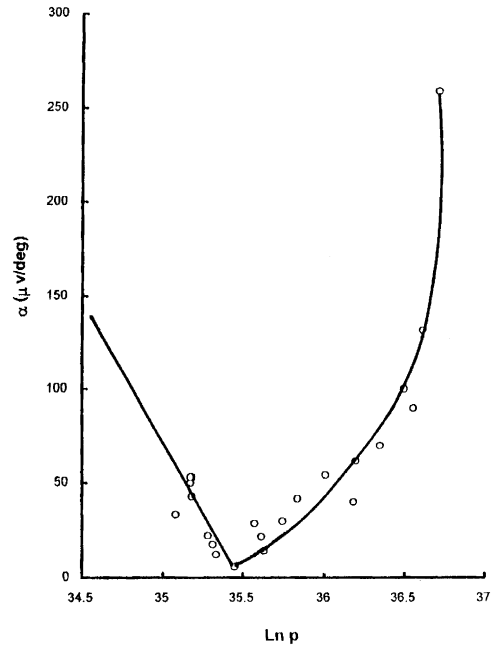


Fig. 9. The relation between α and charge carrier concentration of Ga_2Te_5 .

estimated to be $\tau_p = 2.58 \times 10^{-13} \text{ s}$ and $\tau_n = 8.03 \times 10^{-16} \text{ s}$. By using the values of diffusion coefficient and the mean free time, the diffusion length for both charge carriers can be determined. The values of the diffusion length for electrons and holes are found to be $L_n = 4.15 \times 10^{-7} \text{ cm}$ and $L_p = 5.58 \times 10^{-6} \text{ cm}$, respectively.

Fig. 10 shows the dependence of thermoelectric power coefficient α on the natural logarithm of electrical conductivity according to [21]:

$$\alpha = \frac{K}{e} \left[A + \ln \frac{2(2\pi m_p^* KT)^{3/2}}{(2\pi h)^3} \right] - \frac{K}{e} \ln \sigma. \quad (4)$$

It seems that the TEP decreases, reaches a lower value of $5 \mu\text{V}/\text{K}$ and then it increases gradually and slowly as electrical conductivity increases. The behaviour of α in the high conductivity region may be due to the high value of carrier concentration in these ranges. On the other hand, the decrease of α with σ in the low conductivity region can be attributed to the increase in both carrier density and its mobility. The high value of α in the low

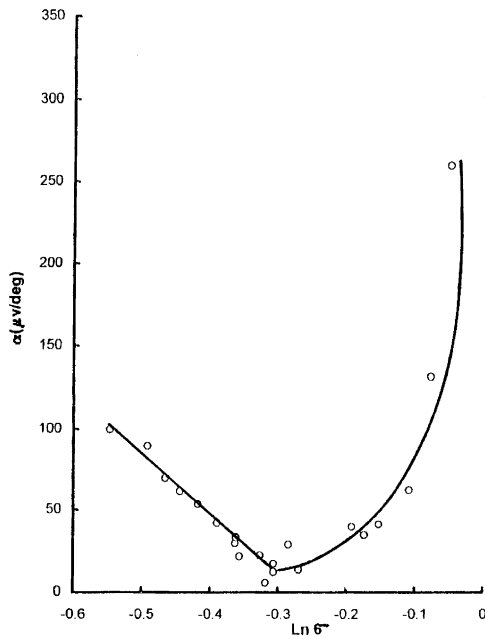


Fig. 10. Variation of thermoelectric power with conductivity for Ga_2Te_5 .

conductivity region indicates drag of carriers by phonons.

References

- [1] P.C. Newman, J.C. Brice, H.C. Wright, Philips Res. Rept. 16 (1961) 14.
- [2] F. Alapini, J. Flahaut, M. Guittard, S. Jaulmes, M. Julien-Pouzol, J. Solid State Chem. 28 (1979) 309.
- [3] J.R. Dale, Nature 197 (1963) 242.
- [4] M. Hansen, K. Anderko, Constitution of Binary Alloys, McGraw-Hill, New York, 1958.
- [5] W. Klemm, H.U.V. Vogl, Z. Anorg. Allg. Chem. 219 (1934) 45.
- [6] J.G. Antonopoulos, T.H. Karakostas, G.L. Bleris, N.A. Economou, J. Mater. Sci. 16 (1981) 733.
- [7] R. Blachnik, E. Irle, J. Less-Common Met. 113 (1985) L₁.
- [8] K.U. Tschirner, B. Garlipp, R. Rentzsch, Z. Metallkd. 77 (1986) 811.
- [9] Y. Lenvinsky, G. Effenberg, S. Ilenko, Pressure Dependent phase Diagrams of Binary Alloys, ASM International, Materials Park, OH, USA, 1997.
- [10] Hiroaki Okamoto, P.R. Subramanian, L. Kacprzak, Binary Alloy Phase Diagrams, ASM International, Materials Park, OH, USA, 1990.
- [11] H.J. Deiseroth, P. Amann, Z. Anorg. Allg. Chem. 622 (1996) 985–993.
- [12] D.W. Bullett, Solid State Commun. (USA) 51 (1984) 1.
- [13] S.A. Hussein, A.T. Nagat, published in Cryst. Res. Technol, 1989.
- [14] S.A. Hussein, Cryst. Res. Technol. 24 (6) (1989) 635.
- [15] G.A. Gamal, M.M. Nassary, S.A. Hussein, A.T. Nagat, Cryst. Res. Technol. 27 (5) (1992) 629–635.
- [16] N. Cusack, The Electrical and Magnetic Properties of Solids, Longman and Green, New York, 1958.
- [17] H.A. Elshaikh, G.A. Gamal, Semicond. Sci. Technol. 10 (1995) 1034–1036.
- [18] J. Lauc, J. Phys. Rev. 95 (1954) 1394.
- [19] P.S. Kireev, Semiconductor Physics, Mir Publishers, Moscow, 1974.
- [20] A.H. Wilson, Theory of Metals, 2nd Edition, Cambridge University Press, Cambridge, 1953.
- [21] P.H.E. Schmid, E. Mooser, Helv. Phys. Acta. 45 (1972) 870.